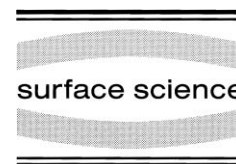




ELSEVIER

Surface Science 402–404 (1998) 764–769



The Ir(110) surface studied by STM

J. Kuntze *, S. Speller, W. Heiland

Universität Osnabrück, FB Physik, D-49069 Osnabrück, Germany

Received 26 August 1997; accepted for publication 1 October 1997

Abstract

The Ir(110) surface is studied by STM, assisted by LEED and AES. The clean surface exhibits a mesoscopic “rippling” due to formation of (331) facets, confirming former results. The “ridges” formed by the inclining and declining facets are up to several 100 Å long in $[1\bar{1}0]$ direction and have an average width of approximately 40 Å, resulting in a quite rough topography on a mesoscopic scale. At the top of the ridges a close packed double row separating the facets has been found. The Ir(110) surface is the only known fcc(110) surface that exhibits stabilization via (331) facets, whereas Au(110) and Pt(110) reconstruct in the (1×2) missing row structure with (111) facets. © 1998 Elsevier Science B.V. All rights reserved.

Keywords: Iridium; Low index single crystal surfaces; Scanning tunneling microscopy (STM); Surface structure

1. Introduction

The investigation of fcc(110) surfaces has been of great interest for many years. For Au(110) and Pt(110) it is known that the clean surfaces show a (1×2) missing row reconstruction [1–7]. For the Ir(110) surface, however, the structure of the clean surface is still a matter of research. Early results favoured a (1×2) missing row reconstruction as for Au and Pt [8–10]. Hetterich et al. have found [11] that this may be due to Si impurities and state, along with other studies, that the structure of the clean surface is (1×3) [12–16]. However, in the last years STM studies by Koch et al. [17, 18] and He atom diffraction by Avrin and Merrill [19] have shown that the structure may still be different. They obtain the unexpected result that Ir(110) tends to stabilize via (331) facets, which leads to

mesoscopic “rippling” of the surface. Up to now these two groups have been the only ones who reported this novel kind of surface stabilization.

2. Experimental set-up and preparation

We used scanning tunneling microscopy (STM), supported by low energy electron diffraction (LEED) and Auger electron spectroscopy (AES). Our STM is an OMICRON-STM-1 described in detail elsewhere [20]. The STM piezos were calibrated using the (7×7) -reconstructed Si(111) surface and the Pt(110) (1×2) surface. All STM images shown here are taken at room temperature. Surface preparation is done by sputtering with 500 eV Ar^+ ions ($I \approx 5 \mu\text{A}$) followed by annealing to approximately 1000 K. The setpoint temperature was reached within 10 min and held for 10–20 min; cooling down took 30–90 min. The

* Corresponding author.
E-mail: jens.kuntze@rz.uni-osnabrueck.de

heating was done with a tantalum filament placed behind the sample holder. Temperatures were measured via a pyrometer and a thermocouple fixed at the manipulator head near the sample. No oxygen treatments were used to clean the surface in order to avoid the formation of oxides of possible contaminants as Si or Ca.

3. Results and discussion

After several sputtering and annealing cycles the contamination of the sample was below the detection limit of AES (compare spectrum in Fig. 1) and showed a “streaky” LEED pattern (Fig. 2), which can be explained with a faceting of the surface. The intensity distribution varies in a complex manner when changing the electron energy, and the spots seem to move independently towards and off the centre of the screen.

A closer look at the pattern at 237 eV (lower panel of Fig. 2) reveals the regular array of spots in the [001] azimuth (horizontal direction in the pattern), in which the separation of the beams

corresponds to a distance of $6 \pm 0.5 \text{ \AA}$, which is in excellent agreement with the typical distance of 5.76 \AA along the sides of the facets (Fig. 3).

Even the centered symmetry of a (331) facet is present in all the patterns, but most clearly in the pattern at 273 eV.

The pattern at 158 eV (upper panel in Fig. 2) also reproduces quite well the intensity distribution shown in Ref. [18] at 156 eV. It demonstrates the complexity of the intensity distribution along the [001] azimuth: the narrow spots at both sides of the electron gun seem to merge and split again when the energy is increased only a few electron volts. This gives rise to complex intensity variations, and only at certain energies is a “simple” pattern observed, which sometimes reminds us of a (1×3) symmetry.

The STM topography shows on a mesoscopic scale a “rippled” surface (Fig. 4). The “ridges” running along the $[1\bar{1}0]$ direction are up to several hundred ångströms long and have a width of $30\text{--}50 \text{ \AA}$ (see height scan below the image). Sometimes even larger facets are observed. A width of approximately 40 \AA seems to be most favourable, which is larger than the value obtained by

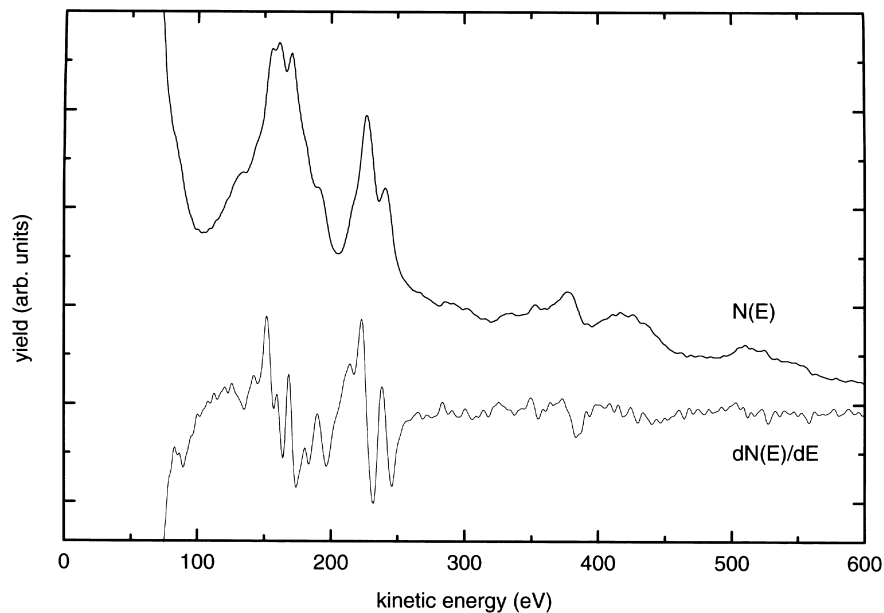


Fig. 1. AE spectrum of the Ir(110) surface. The top line represents the energy spectrum, the bottom line the first derivative.

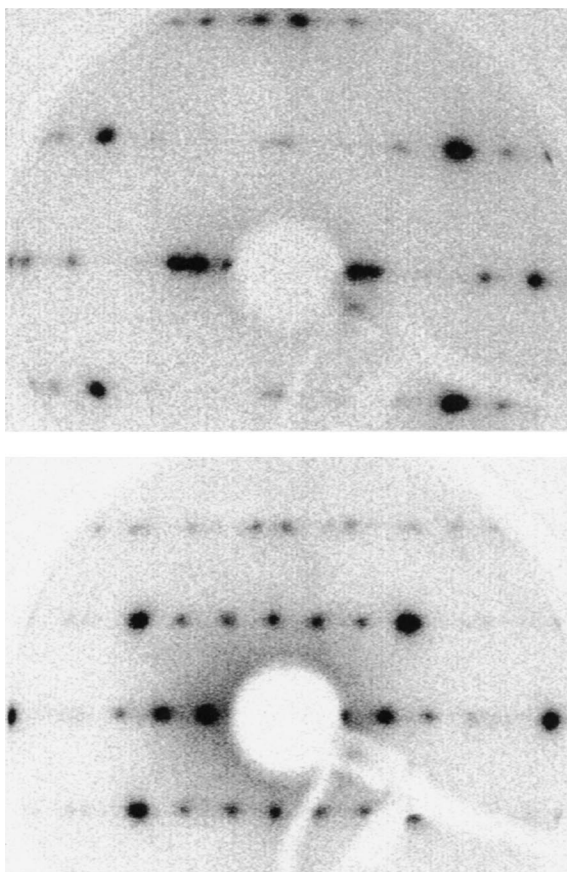


Fig. 2. LEED pattern of the microfaceted Ir(110) surface, taken at 158 eV (top) and 273 eV (bottom).

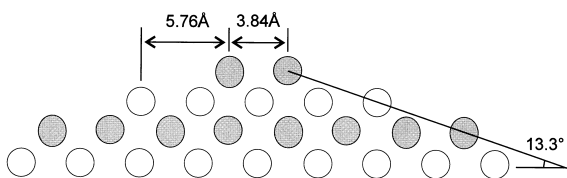


Fig. 3. Model of a single "ridge". The inclination of the (331) and $(3\bar{3}\bar{1})$ facets is 13.3° versus the (110) plane, which lies parallel to the two close packed $[1\bar{1}0]$ rows at the top of the ridge. The lateral distance of the outermost atoms at the sides is 5.76 Å.

He diffraction, where 18 \AA was found to be most pronounced [19]. Compared to the other 3d-transition metals the $[1\bar{1}0]$ rows seem more stable and the disorder is higher perpendicular to the rows.

On a small scale it can be seen (Fig. 5) that these "ridges" consist of several $[1\bar{1}0]$ rows in successively higher layers separated by $\approx 3a_0/2$ in $[001]$ direction, where $a_0 = 3.84 \text{ \AA}$ is the lattice constant of the crystal. This results in inclinations of the facet between 10 and 15° , which is close to the theoretical expected value of 13.3° for (331) facets. A (111) facet would incline at a much steeper angle of 35.3° and would not exhibit these small "bumps" at the sides separated by $3a_0/2$. At the top of the facet shown in Fig. 5 a close packed double row can be seen. This seems to be an inherent feature of the structure, since we always notice such a double row at the top in accordance with the findings of refs. [17,18]. Although it may appear critical to measure the exact distances and inclination angles because of the difficulty of appropriate background subtraction [there is no evident "reference" plane that can be regarded as parallel to the (110) plane, and the two close packed rows at the top of the facets define a rather small "terrace"] the measured values are close to the calculated values, far from experimental error.

We observed no critical preparation conditions under which this special reconstruction occurs, provided that the surface is being annealed high enough (at least 800 K). Longer annealing and/or slower cooling did not improve the LEED pattern or considerably alter the mesoscopic distribution of the ridges seen by STM. However, the length of the ridges shortened with increasing contaminations like C or Ca that sometimes appeared upon high annealing and the mesoscopic topography was even more rough. Since we did not anneal the sample in an oxygen atmosphere, did not use flashing to high temperatures and in general annealed only for a quite limited time of 10–20 min, segregation of impurities should be minimized. If the faceted reconstruction is caused by impurities, these must be present in very low concentration and additionally be typical contaminants in iridium crystals, since this structure has been reported now by three independent groups. The observed correlation between Si and/or SiO signals in the AE spectra and a (1×2) LEED pattern [11] exclude these two contaminants as stabilizers for the faceted structure.

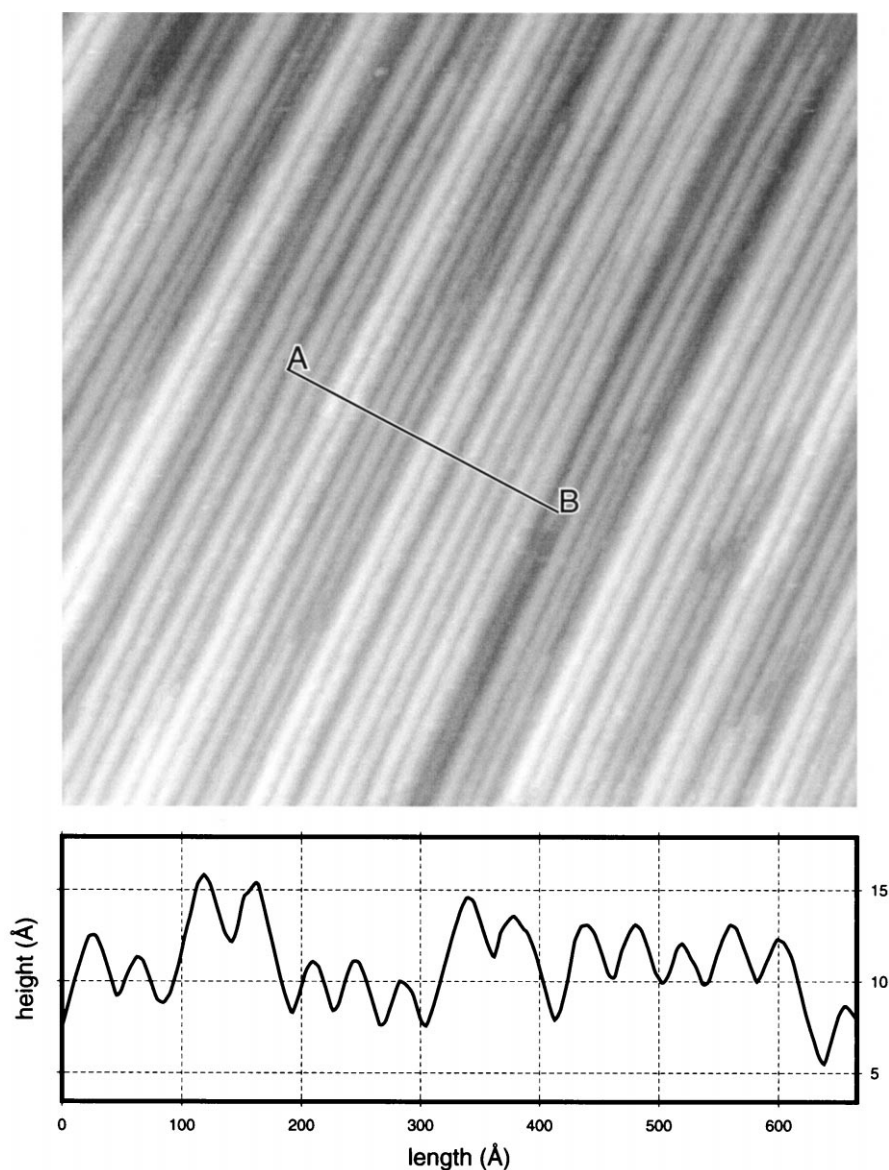


Fig. 4. Overview STM topograph $2000 \times 2000 \text{ \AA}^2$, $U_t = 0.93 \text{ V}$, $I_t = 1.0 \text{ nA}$. The height scale corresponds to 40 \AA . The $[1\bar{1}0]$ direction is parallel to the row-like facets. The height scan below the image indicates an average facet width of approximately 40 \AA . The inclination of the sides of the “ridges” is $10^\circ\text{--}15^\circ$, which is in reasonable agreement with the expected 13.3° for (331) facets.

Adsorbed oxygen is known as a stabilizer for the (1×1) and the $c(2 \times 2)$ structure [8,9,14,18,21,22]. Ca deteriorates the formation of the faceted structure and tends to induce (1×3) patches [23]. Sulphur also induces different reconstructions, which we checked by annealing the sample after adsorbing a monolayer of H_2S [24].

The role of other possible contaminants such as, for example, K and P should be more carefully addressed in future research. But since no study reporting the faceted reconstruction mentions significant amounts of these impurities, their influence may be marginal, and the driving force for this structure must be sought elsewhere.

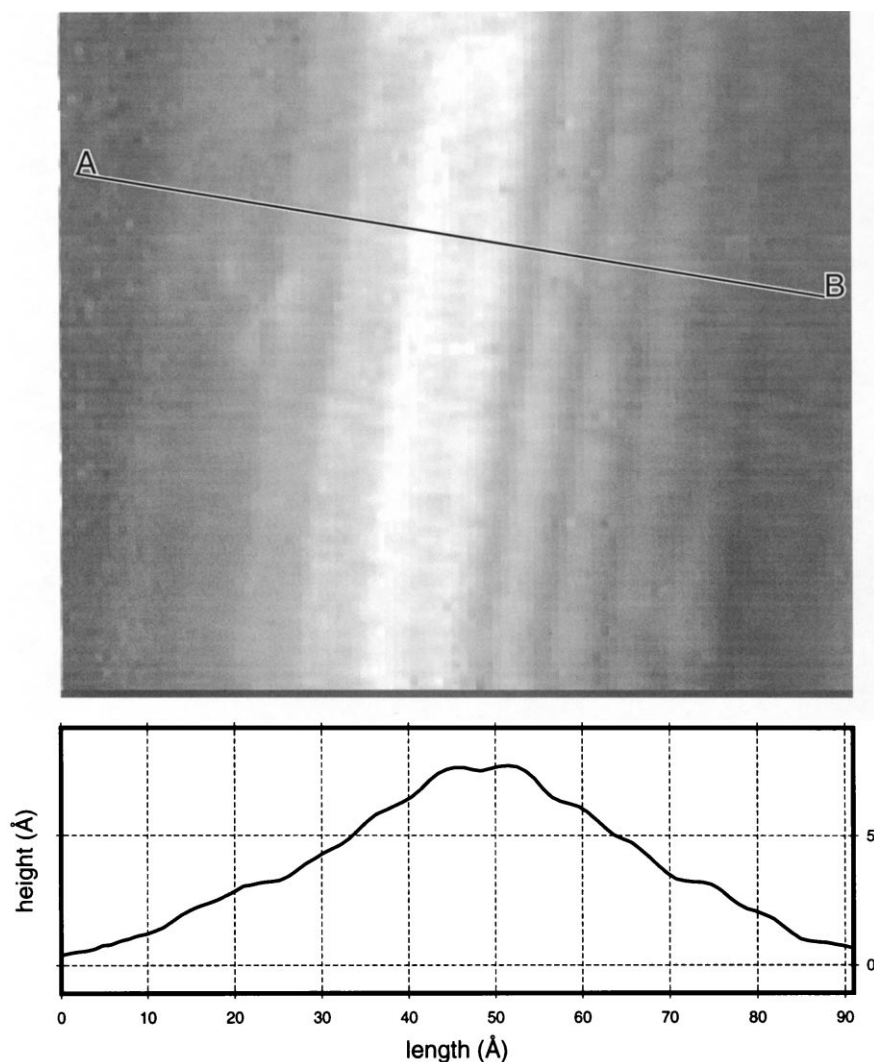


Fig. 5. STM topograph of one of the “ridges” $95 \times 82 \text{ \AA}^2$, $U_t = -0.3 \text{ V}$, $I_t = 1.0 \text{ nA}$. The height scale corresponds to 10 \AA . Slight differentiation has been used to enhance contrast. The height scan along the $[001]$ direction clearly indicates the two close packed $[1\bar{1}0]$ rows at the top of the ridge and the small “bumps” at the sides at a lateral distance of $7 \pm 1 \text{ \AA}$ correspond to rows in successively deeper layers, resulting in an inclination of the walls of approximately 10° , in agreement with the (331) faceted model in Fig. 3.

In a recent *ab initio* study on Ir(110) [25] a (1×2) reconstruction was found to be favourable compared to the relaxed, unreconstructed surface. The main reason for this prediction is the energy gain upon reconstruction, whereas surface stress was found to be even higher in the (1×2) case. This may be different for the (331) microfaceted model with mesoscopic rippling. Since the relief of surface stress has been considered as a driving

force for the large scale periodic hill-and-valley structure found on clean Pt(110) [26], and also for several other mesoscopic patterns on semiconductors [27–30] and metal–adsorbate systems [31–33], it may also play a role in the formation of the rippling on Ir(110). In this picture the observed period of 40 \AA may lead to the assumption that the intrinsic stress on Ir(110) is considerably higher than that on Pt(110), where much larger structures

with a period of 1500 Å have been found. It must be asked, however, if the approaches using continuum elastic theory are still applicable for the rather small structures of Ir(110). We hope that theoretical studies may be inspired to undertake new efforts to calculate the energetics of this structure.

Acknowledgements

Financial support by the Deutsche Forschungsgemeinschaft (DFG) is gratefully acknowledged.

References

- [1] D.G. Fedak, N.A. Gjostein, *Acta Metall.* 15 (1967) 827.
- [2] H.P. Bonzel, R. Ku, *J. Vacuum Sci. Technol.* 9 (1972) 663.
- [3] P. Fery, W. Moritz, D. Wolf, *Phys. Rev. B* 38 (1988) 7275.
- [4] E.C. Sowa, M.A. Van Hove, D.L. Adams, *Surf. Sci.* 199 (1988) 174.
- [5] P. Fenter, T. Gustafsson, *Phys. Rev. B* 38 (1988) 10197.
- [6] E. Vlieg, I.K. Robinson, *Surf. Sci.* 233 (1990) 248.
- [7] U. Korte, G. Meyer-Ehmsen, *Surf. Sci.* 271 (1992) 616.
- [8] K. Christmann, G. Ertl, *Z. Naturforsch.* 28a (1973) 1144.
- [9] J.L. Taylor, W.H. Weinberg, *Surf. Sci.* 79 (1979) 349.
- [10] M.A. Van Hove, W.H. Weinberg, C.-M. Chan, *Low-Energy Electron Diffraction*, Springer Series in Surface Sciences 6, Springer, Berlin, 1986.
- [11] W. Hetterich, U. Korte, G. Meyer-Ehmsen, W. Heiland, *Surf. Sci.* 254 (1991) L487.
- [12] W. Hetterich, W. Heiland, *Surf. Sci.* 210 (1989) 129.
- [13] H. Bu, M. Shi, F. Masson, J.W. Rabalais, *Surf. Sci.* 230 (1990) L140.
- [14] H. Bu, M. Shi, J.W. Rabalais, *Surf. Sci.* 236 (1990) 135.
- [15] W. Hetterich, W. Heiland, *Surf. Sci.* 258 (1991) 307.
- [16] C. Höfner, W. Hetterich, H. Niehus, W. Heiland, *Nucl. Instrum. Meth. Phys. Res. B* 67 (1992) 328.
- [17] R. Koch, M. Borbonus, O. Haase, K.H. Rieder, *Phys. Rev. Lett.* 67 (1991) 3416.
- [18] R. Koch, M. Borbonus, O. Haase, K.H. Rieder, *Appl. Phys. A* 55 (1992) 417.
- [19] W.F. Avrin, R.P. Merrill, *Surf. Sci.* 274 (1992) 231.
- [20] S. Speller, T. Rauch, W. Heiland, *Surf. Sci.* 342 (1995) 224.
- [21] C.-M. Chan, S.L. Cunningham, K.L. Luke, W.H. Weinberg, S.P. Withrow, *Surf. Sci.* 78 (1978) 15.
- [22] C.-M. Chan, K.L. Luke, M.A. Van Hove, W.H. Weinberg, S.P. Withrow, *Surf. Sci.* 78 (1978) 386.
- [23] J. Kuntze, J. Bömermann, T. Rauch, S. Speller, W. Heiland, *Surf. Sci.* 394 (1997) 150.
- [24] J. Kuntze, S. Speller, W.H. Heiland, in preparation.
- [25] A. Filippetti, V. Fiorentini, *Surf. Sci.* 377/379 (1997) 112.
- [26] P. Hanesch, E. Bertel, *Phys. Rev. Lett.* 79 (1997) 1523.
- [27] J. Tersoff, R.M. Tromp, *Phys. Rev. Lett.* 70 (1993) 2782.
- [28] C. Teichert, M.G. Lagally, L.J. Peticolas, J.C. Bean, J. Tersoff, *Phys. Rev. B* 53 (1996) 16334.
- [29] O.L. Alerhand, D. Vanderbilt, R.D. Meade, J.D. Joannopoulos, *Phys. Rev. Lett.* 61 (1988) 1973.
- [30] D.E. Jones, J.P. Pelz, *Phys. Rev. Lett.* 75 (1995) 1570.
- [31] K. Kern, H. Niehus, A. Schatz, P. Zeppenfeld, J. Goerge, G. Comso, *Phys. Rev. Lett.* 67 (1991) 855.
- [32] H. Hörnis, J.D. West, E.H. Conrad, *Phys. Rev. B* 48 (1993) 14577.
- [33] H. Niehus, C. Achete, *Surf. Sci.* 369 (1996) 9.